Accepted Manuscript

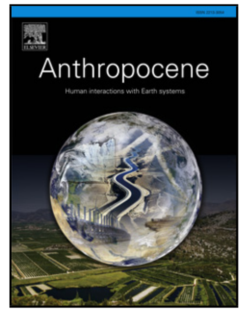

Title: Anthropocene Metamorphosis of the Indus Delta and Lower Floodplain

Author: James P.M. Syvitski Albert J. Kettner Irina Overeem Liviu Giosan G. Robert Brakenridge Mark Hannon Roger Bilham

PII: S2213-3054(14)00005-8
DOI: http://dx.doi.org/doi:10.1016/j.ancene.2014.02.003
Reference: ANCENE 26

To appear in:

Received date: 15-9-2013
Revised date: 15-2-2014
Accepted date: 17-2-2014

Please cite this article as: James P.M. SyvitskiAlbert J. KettnerIrina OvereemLiviu GiosanG. Robert BrakenridgeMark HannonRoger Bilham Anthropocene Metamorphosis of the Indus Delta and Lower Floodplain (2014), http://dx.doi.org/10.1016/j.ancene.2014.02.003

Anthropocene Metamorphosis of the Indus Delta and Lower Floodplain

James P.M. Syvitski[1], Albert J. Kettner[1], Irina Overeem[1], Liviu Giosan[2], G. Robert Brakenridge[1], Mark Hannon[1], Roger Bilham[2]

1. CSDMS/INSTAAR, U. Colorado, Boulder CO, 80309-0545, James.syvitski@colorado.edu
2. Geology and Geophysics, Woods Hole Oceanographic Institution, Woods Hole, MA 02543
3. CIRES and Geological Sciences, U. Colorado, Boulder CO, 80309-0399

Abstract

The Indus River/Delta system is highly dynamic, reflecting the impacts of monsoonal-driven floods and cyclone-induced storm surges, earthquakes ranging up to Mw=7.8, and inundations from tsunamis. 19th century Indus discharge was likely larger than today, but upstream seasonal spillways limited the maximum flood discharge. Upstream avulsions during the 2010 flood similarly reduced the downstream discharge, so that only 43% of the floodwaters reached the delta. The present-day Indus River is wider with larger meander wavelengths (~13 km) compared to the 4km to 8km meander wavelengths for the super-elevated historical channel deposits. The Indus River is presently affected by: 1) artificial flood levees, 2) barrages and their irrigation canals, 3) sediment impoundment behind upstream reservoirs, and 4) inter-basin diversion. This silt-dominated river formerly transported 270+ Mt/y of sediment to its delta; the now-transformed river carries little water or sediment (currently ~13 Mt/y) to its delta, and the river often runs dry. Modern-day reduction in fluvial fluxes is expressed as fewer distributary channels, from 17 channels in 1861 to just 1 significant channel in 2000. Abandoned delta channels are being tidally reworked. Since 1944, the delta has lost 12.7 km^2/y of land altering a stunning 25% of the delta; 21% of the 1944 delta area was eroded, and 7% of new delta area formed. The erosion rate averaged ~69 Mt/y, deposition averaged ~22 Mt/y, providing a net loss of ~47 Mt/y particularly in the Rann of Kachchh area that is undergoing tectonic subsidence.

Anthropocene Metamorphosis of the Indus Delta and Lower Floodplain

Abstract

The Indus River/Delta system is highly dynamic, reflecting the impacts of monsoonal-driven floods and cyclone-induced storm surges, earthquakes ranging up to Mw=7.8, and inundations from tsunamis. The 19th century Indus discharge was likely larger than today, but upstream seasonal spillways limited the maximum flood discharge. Upstream avulsions during the 2010 flood similarly reduced the downstream discharge; only 43% of floodwaters reached the delta. The present-day Indus River is wider with larger meander wavelengths (~13 km) compared to the 4km to 8km meander wavelengths for the historical channel deposits. The Indus River is presently affected by: 1) artificial flood levees, 2) barrages, 3) sediment impoundment behind reservoirs, and 4) inter-basin diversion. The Indus formerly transported 270+ Mt/y of sediment to its delta; the river now delivers little water or sediment (currently ~13 Mt/y); the river often runs dry. Reduction in fluvial fluxes is expressed as fewer distributary channels, from 17 in 1861 to 1 significant channel in 2000. Abandoned delta channels are being tidally reworked. Since 1944, the delta has lost 12.7 km^2/y of land altering 25% of the delta. Erosion averaged ~69 Mt/y, deposition averaged ~22 Mt/y, providing a net loss of ~47 Mt/y particularly in the Rann of Kachchh a tectonic subsiding area. The former river-delta system likely could not be converted back to its pre-Anthropocene state. The Indus River's self-regulating processes have not buffered these changes, and have initiated self-enhancing mechanisms. These lessons are globally applicable to other delta systems (e.g. Mississippi, Colorado, Ganges, Po, and Nile).

Introduction

Among the world's large deltas, the Indus has been one of the more dynamic systems, reflecting its large, tectonically active mountain belt upland, the impacts of monsoonal-driven floods and cyclone-induced storm surges, nearby historical tectonic events (e.g. earthquakes ranging up to Mw=7.8), and inundations from tsunamis. Some human interventions are ancient, dating back some 4000 years before present. However it is during the past 150 years that the river and its delta have experienced human interventions as a geomorphic factor of consequence (e.g. watershed deforestation, diversion canals, and dams, levees and barrages that today comprise the world's largest irrigation system). *This paper contrasts the evolution of the Indus River-delta system under mid-Holocene (post 6,500 yr B.P.) conditions, to its evolution through the 20th century*. In the 19th and 20th century, human impact on the Holocene river system changed to such extent that dubbing the last centuries the 'Anthropocene' is appropriate. During the Late Holocene, river avulsions both transient and permanent were normal, and multiple distributary channels fed an actively prograding tide- and wave-affected delta. Natural avulsions were still occurring in the 19th century. During the present Anthropocene, flood deposition and avulsions are restricted by engineering works, water and sediment flux to the coastal ocean is greatly reduced, and coastal retreat, tidal-channel development, salinization of irrigated soils, and saltwater intrusion have all occurred. *We seek to quantify these changes and infer their proximal causation. In particular, how has the long-term 'harnessing' of this river affected its large-scale geometry, and its floodplain deposition; how has sediment and water starvation affected the delta fringe?* The enormity of this geo-engineering experiment offers many lessons. Our analysis includes data on channel patterns from geo-located historical maps over the 19th and 20th century with reference to earlier times, satellite imagery collected during the last 35 years, and satellite-based flood inundation surveys.

Environmental Setting

The Indus fluvio-deltaic lowlands receive water, sediment and nutrients from the 1 M km^2 Indus drainage basin. Before human intervention in the 20th century, average discharge for the 2900 km long Indus River was 3000 m^3/s and it carried a silty sediment load of at least 250 Mt/y (Milliman et al., 1984). The more pristine Indus had an unusually high suspended sediment concentrations ~3 kg/m^3 (Holmes, 1968). Peak discharge can exceed 30,000 m^3/s, commonly during July-September, and are driven by heavy monsoon rains. Annual rainfall ranges from frontal Himalayan values of almost 200 cm to only ~23 cm on the Indus plain, and even lower values (~9 cm) over the Indus Delta.

Tectonics control the container valley geometry of the Indus, and the main course of the Indus migrated to a generally more westward located course over the past 5000 years (Kazmi, 1984). The legendary Saraswati River, whose probable ancient course in the Thar Desert is marked by numerous abandoned archaeological sites, may have once supplemented the Indus delta (Oldham, 1886; 1893; Stein, 1942; Lal and Gupta 1984; Mughal 1997; Giosan et al. 2012). Rather than being an effect of Saraswati's loss, we speculate that a westward migration of the Indus course may have a more deep seated cause, possibly associated with slow flexural uplift of the central Indian plateau (Bilham et al., 2003).

The delta's climate is arid sub-tropical; the river mouth is located almost in the tropics, at 24° N 67°30' E. The present Indus delta is 17,000 km^2; the active tidal flat area is ~10,000 km^2. The delta once hosted the world's largest arid mangrove forest (Inam et al, 2007). Warm coastal waters (22°C on average) and summer tidal inundation result in salt deposits (Memon 2005). The tidal range is 2.7m (Giosan et al 2006). Swampy areas on the delta are restricted to areas near tidal channels and coastal areas that undergo tidal flooding.

Although the Indus delta receives high deep-water wave energy, attenuation on the shallow shelf results in lower wave energy at the coast than is typical for wave-dominated deltas (Wells and Coleman, 1984). Wave measurements offshore Karachi at 20 m water-depth show a mean significant wave height during the summer southwest monsoon (May–September) of ~ 1.8m with a mean period of 9 s (Rizvi et al. 1988). During the winter, with offshore-directed monsoon winds (October–April), significant wave height is ~ 1.2m with a period of 6.5 s (Rizvi et al., 1988). Wave-driven sediment transport redistributes river-delivered sediments along the deltaic coast (Wells and Coleman, 1984; Giosan et al., 2006).

The Indus and its Lower Floodplain

The More Natural Indus River

Recorded regional history extends back several thousand years (including annals from the time of Alexander the Great c. 325 BC). Embracing ~2 millennia prior, humans certainly modified the landscape: the population of the Harappan culture is estimated at ~5 million at peak, with ~1000 major settlements in what is now Pakistan. However, we postulate these modifications are relatively minor compared to changes from 1869 onwards when artificial levees and great modern irrigation systems became established, population grew from ~25 million people to the present ~188 million (UN, 2012), and the Indus ceased to transport large quantities of freshwater and sediment to the delta and the sea. We here describe natural processes occurring in the presence of humans, but not so greatly altered by them.

The Indus floodplain (Fig. 1, 2) is between 100-200 km wide and consists of deep deposits of unconsolidated and highly permeable alluvium deposited by the Indus River and its tributaries (Kazmi, 1984). During the Holocene between ~300 and 1100 Mt/y were delivered by the Indus River to its lower alluvial plain and delta (Clift and Giosan, 2013). Immediately before the 20th century damming activities started, the Indus deposited ~60% of its total load along its lower alluvial plain: with more than 600 Mt/y entering the alluvial plain and only 250 Mt/y reached the delta (Milliman et al., 1984). This relationship holds at the scale of the entire Holocene with roughly half of sediment discharge by the river contributing to the aggradation of the lower alluvial plain and subaerial delta and the other half contributing to the progradation of both the subaerial and subaqueous delta (Clift and Giosan, 2013).

Schumm et al. (2002) considers the modern Indus plain to be comprised of two inland alluvial fans, one focused north of Sukkur and the other near Sehwan, with avulsions occurring near the apex of these fans. Based on higher resolution data, we see the floodplain more as a series of prograding and overlapping sediment fans or deposits (Figs. 2A, 2B, 3A) that reflect the movement of the historical Indus River (cf. Fig. 1). Schumm et al. (2002) regards the avulsions to be controlled by tectonics because avulsions appeared to have occurred repeatedly at the same location. The area containing Jacobobad- Khaipur lies close to the frontal folds of the Sulaiman lobe (Szeliga et al., 2010) and hence is influenced by incipient local fold-and thrust tectonics. The area immediately east of Karachi lies near an east-verging fold and thrust belt (Schelling, 1999; Kovach et al., 2010), whereas the eastern delta including the Rann of Kachchh is subject to footwall subsidence associated with reverse faulting of the Kachchh mainland and other faults (Jorgensen et al 1993; Bendick et al., 2001; Biswas, 2005). That natural avulsions were triggered by tectonic events is further evidenced by the fact that Mansurah (25.88°N, 68.78° E), the Arabic capital of the Sindh province, was destroyed by an earthquake c. 980AD (Intensity ≈VIII), resulting in a post-seismic avulsion of the river (Fig. 3 inset, Bilham and Lodi 2010). Since natural levees have been observed in India to collapse during intensity VII shaking, it is unnecessary to invoke co-seismic uplift as a requirement for upstream river avulsion (Bilham and Lodi 2010). A similar possibly modest earthquake that occurred in 1668 in the historical province of Nasirpur destroyed the town of Samawani (Fig. 3) and again initiated avulsion of the Indus main channel (Bilham and Lodi 2010).

Levee breaching during significant flood events is thought to be directly responsible for other historical river avulsions (Holmes, 1968). The relatively coarse sediment load favors formation of new channels rather than reoccupation of older small channels, which silt up quickly to function as secondary spillways (Holmes 1968).

Figure 1 shows paleochannel locations recognized from planview fluvial architectural elements, from visible satellite imagery (LANDSAT, SPOT, DigitalGlobe satellites), and identified from their topographic expression (Syvitski et al., 2012) as reconstructed from the SRTM topography (Fig. 2). Channel names (and their spelling) are from Holmes (1968), who applied forensic historical analysis to determine when these channels would have been most active. Holmes (1968) identified three channel patterns expressed within air photos (Fig. 1): circa 325 BC, 900 AD and 1600 AD. These dates represent generalized periods. Historical maps were analyzed for their spatial geo-location error (Table 1), by digitally identifying towns on geo-referenced maps and comparing them to modern city locations. Maps earlier than 1811 did not have sufficient positioning detail to have their root-mean-square error determined. Few cities lasted across multiple centuries, in part because Indus River avulsions commonly left river settlements without water resources for drinking, agriculture, or transportation. [Note: Sindh towns often changed their spelling and towns that were re-located sometimes kept their old name: see supplementary spelling data].

Pinkerton (1811, see suppl. matl.) notes that the Indus River was navigable from the mouth to the province of Lahore, 900 km upstream for ships of 200 tons. At that time the Indus River system included an extensive set of natural overflow flood pathways across the Indus plain as indicated by Lapie (1829, see suppl. matl.). An SDUK 1838 map shows the Indus flowing on both sides of Bukkur, an island near Sukkur.. The same map indicates that the Indus was typically 500m wide, 12m deep, with a flow of 1.5 m/s (~4,500 to 9,000 m^3/s) and rose 4m during flood (i.e. ~12,000 to 16,000 m^3/s) — values that are similar to those of today.

The Western Nara River, a northern offshoot course of the main Indus, originated near Kashmore (Fig. 1) in pre-historic time and later near Ghauspur (Panhwar, 1969). As the Indus moved west, this distributary was 37 km north of Larkana by 1860 and only 15 km north by 1902, when it was converted into a canal (Panhwar, 1969). Johnson (1861, see suppl. matl.) shows the Eastern Nara River to be a viable secondary pathway of Indus water to the sea through a complex of river channels. In 1859, the Eastern Nara was converted into a perennial canal (Panhwar, 1969). The Indus adopted its present course west of Hyderabad in 1758 when the Nasarpur Course was deserted (Fig. 1) and discharge greatly decreased down the Eastern Nara (Fig. 1). The Fuleti River, a significant discharge branch to the west of Hyderabad through the first half of the 19^{th} century (SDUK 1933; Johnston 1861, see suppl. matl.), became a spillway and occupied the channel of the former Ren River (Fig. 1).

Using aerial photography covering the region, Holmes (1968) recognized 1) meander deposits formed by Holocene trunk river (e.g. pointbar deposits, deserted channels, and abandoned oxbow lakes), and floodplain cover deposits, formed by vertical accretion of fine sediments in slow-moving floodwaters of the basins. Cover deposits are widespread along the flanking zone from

Jacobabad to Manchar Lake, in the southeast around Mirpur Khas and Umarkot, and in the delta (Holmes 1968). The historical Indus River sent off distributaries and small seasonal spillway channels towards its flanks and across the delta. Such smaller-scale channels are characterized by levees rather than by river bars and meander scrolls. Levees of the Ghar and Western Nara (Fig. 1) are ~3 m high due to periodic overspill of their banks and define these 3 km-wide paleochannels.

Narrower channels and shorter wavelength meanders define former courses of the Indus: the Khairpur at between 4km and 8km; Shahdapur at 5km; and the Warah at 6km (Fig. 1). The modern Indus is wider with larger but fewer meanders (~14km wavelength). Sinuosity of the paleo-Indus channels (Figs. 1 and 2) had a range from: 1) Badahri: 1.51, 2) Warah: 1.55, 3) Kandhkot: 1.65; 4) Puran: 1.81, 5) Shahdadkot: 1.99, 6) Eastern Nara: 2.05, 7) Khairpur: 2.33, and 8) Shahdadpur: 2.51. The modern Indus has sinuosity values ranging from 1.1 to 2.0 with a mean value of 1.8 (see discussion below). Paleochannels therefore had similar or sometimes greater sinuosity.

The visible record of paleochannels represents only the last ~1000 years. The remotely sensed topography of Figure 2 perhaps captures some of the longer record of river avulsion and floodplain development and demonstrates how the floodplain aggrades through major avulsions of the trunk Indus. The large channel belt switches leaving behind 1 to 3 m of super-elevated channel belt deposits that shed crevasse-splay fingers and fans interweaving with cover deposits to their sides (Figs. 2-5). An interesting feature of the imaged floodplain topography is its fan-like appearance (Figs. 2, 5). When viewed along valley profiles (Fig. 3), these fan-like waves have a first order wavelength of 29 km, upon which is superimposed a second order set of waveforms with wavelength of ~3.6 km. We suggest that the first order waveform reflect the avulsion frequency of the main Indus River (on the order of several centuries). Major avulsions shift the loci of floodplain deposition suddenly, leaving behind these first-order super-elevated fan lobes (see Fig. 2B). Whereas the second-order scale features perhaps relate to decadal occurrence of floods that build up intermingled crevasse deposits around the larger paleochannel features (Fig. 5). The width and depth of the modern Indus and other paleochannels are well demonstrated in both strike sections (Fig. 4) and plan view (Fig. 5). [Note: the February 2000 SRTM shuttle topographic survey was collected at a time when much of the Indus was a dry bed river]. Radiocarbon-dated fluvial deposits of old channel belts in lower Sindh indicate that aggradation on the megaridge was minimal during the late Holocene. This relative stability of the late Holocene landscape suggests that the abandoned Khaipur and maybe the Western Nara courses are likely older than ~2700 years and secondary in importance in historical times (Giosan et al. 2012).

The complex processes occurring along the Holocene Indus must, as well, have occurred in the context of environmental and climate variability. Pollen studies from a core recovered from the Arabian Sea off the Makran Coast (24° 509N, 65° 559E; 695 m depth) show an end of more humid conditions, linked to a weakening of the monsoon, between 4700 and 4200 BP (Ivory and Lézine, 2009). From tree ring analysis, Ahmed and Cook (2011) conclude, as regards to current water supply along the Indus: "Perhaps the most worrying feature in the streamflow reconstruction is the occurrence of a pronounced and prolonged 112 year low-flow period from AD 1572 to 1683 (median: 3,404 m^3/s) and a shorter but much drier 27 year period from AD 1637 to 1663 (median: 3,292 m^3/s). The former is ~7% below and the latter ~10% below the median of the observed discharge record". These initial inferences and numerical estimates form a useful Holocene context to the larger changes of the Anthropocene; they constitute the "natural" environmental variability on top of which the human-driven changes are occurring.

The Anthropocene River

The Indus River presently feeds the world's largest irrigation system (Fahlbusch et al. 2004). The Pakistan irrigation system is comprised of 3 major storage reservoirs, 19 barrages, and 43 major canals with a total conveyance length of 57,000 km. There are 89,000 watercourses with a running length of more than 1.65 million km (Inman et al. 2007). Major modifications to natural flows started as early as 1762 when the Phuram River at Mora was dammed as an act of aggression by Ghulam Shah Kalora to destroy crop production in the Rann of Kachchh. The Mora Bund apparently still permitted seasonal flow of the river and additional dams were constructed downstream until in 1783, when the Aly Bundar dam successfully closed the southward egress of the eastern Nara to the sea at Lakput. River traffic between 1762 and 1826 was undertaken by barges between the dams until a flood destroyed all the dams in 1826, including the natural Allah Bund (a reverse fault scarp ridge) associated with the 1819 earthquake (Burnes, 1828). Development of the modern system began in 1859 when the Eastern Nara Canal, from Sukkur to the Eastern Nara River, changed the Eastern Nara from an overflow channel into a perennial branch of the Indus.

The human footprint includes:

1. Construction of artificial levees to protect agricultural lands from inundation by floodwaters of the Indus, which started in 1869 near Sukkur (Asianics Agro-Dev 2000). By the time the Sukkur Barrage was constructed in 1932, the eastern bank included a complete line of bunds from the Sindh/Punjab border to Sehwan, and continuing 1500 km all the way to the Indus delta (Asianics Agro-Dev 2000). With the completion of the Kotri Barrage in 1955, associated flood bunds constricted the active Indus River to a floodplain only 7 to 15 km wide. The Indus fluvio-deltaic system was harnessed and constricted to a single channel.
2. Construction of the barrages and associated irrigation canals has led to a systematic abstraction of water from the Indus River. Twenty-three barrages offer a diversion capacity of 69,500 m^3/s (Asianics Agro-Dev 2000). The 1932 Sukkur Barrage (Fig. 1) can divert 1642 m^3/s (Inman et al. 2007). The 1955 Kotri Barrage (Fig. 1) increased diversion capacity by 992 m^3/s. The 1962 Gudu Barrage increased capacity of 1,281 m^3/s (Inman et

al. 2007). Canals often follow former river courses or floodways.

3. Storage capacity of all dams in the Indus basin is more than 23 km^3; the Warsak Dam and Mangla dam, completed in 1960 and 1967 respectively, have a combined storage of ~10 km^3; the 1974 Tarbela dam adds another ~14 km^3 (ICOLD, 1998).
4. The average pre-Anthropocene annual inflow to the Indus River system was ~220 km^3/y, but 42 km^3/y of the upper Indus eastern rivers is now diverted to India and the total average abstraction of Indus water for irrigation and other uses is 129 km^3/y (Asianics Agro-Dev 2000). Of the remaining water, 96.8% is used for agricultural purposes (in 2002), 1.6% is for domestic use and another 1.6% for industrial use (Inman et al. 2007). Groundwater withdrawal for agriculture is estimated at 6.2 km^3/y (Inman et al. 2007).

The Indus of the Anthropocene is a completely manipulated hydrological system (Syvitski and Brakenridge, 2013), constrained by levees that have greatly changed both form and function of the river when compared with earlier channel belts. To examine the effects of these changes in more detail, we consider the evolution of river channel sinuosity and lateral migration rates.

Sinuosity is the ratio of thalweg length to river valley length, using appropriate length scales (Knighton 1998). Migration rates are determined from changes in thalweg position between any two time-intervals, for example every 2 km along the Indus River. We use the years 1944 (USACE 1944 maps; with a geolocation RMS error 196 m, Table 1), 2000 (SRTM, RMS error 55 m, Table 1) and 2010 pre and post-flood data (MODIS, RMS error 50 m). Figure 1 provides the 1944, 2000 and post-flood 2010 Indus thalweg. The 1944 data are from Survey of India Maps updated with aerial photography by Army Map Service (USACE 1944 & suppl. matl.). The 1944 maps predate a 70% reduction of water discharge and an 80% reduction of its sediment load that followed a major increment in the emplacement of barrages and dams Milliman et al. 1984). We contrast these migration rates so determined, with those resulting from the 2010 flood on the

Indus River when ~40,000 km^2 of floodplain was inundated and 20 million Pakistani citizens were displaced, accompanied by 2000 fatalities (Syvitski and Brakenridge, 2013).

The fluvial reach of the Indus River below Sukkur exhibited a sinuosity of 1.63 in 1944. Sinuosity was 1.81 in 2000 and 1.82 by 2010 (pre-flood). After the 2010 river flood, sinuosity decreased to 1.71 in just two months. Pakistan has experienced severe floods in 1950, 1956, 1957, 1973, 1976, 1978, 1988, 1992 and 2010 (Hashmi 2012). The lateral migration between 1944 and 2000 was 1.95 ± 0.2 km on average (Fig. 6), a rate of 36 m/y, but only 14 m/y between the 2000 and 2010 pre-flood imagery. Remarkably during the 2010 flood, the lateral migration rate averaged 339 m in just 52 days, or 6.5 m/d. This rate suggests that the action of decadal flood events is the dominant control on the long-term migration and reworking of a channel belt.

Sinuosity in the portion of the delta plain river influenced by tidal pumping (downstream of Thatta, Fig. 1) was 1.48 in 1944, 1.65 in 2000 (an increase of 35%), 1.75 in 2010 pre-flood and 1.70 in post-flood 2010. Similar to the fluvial-only reach, the tidal influenced portion of the river's sinuosity decreased by 7%. Lateral migration rates between 1944 and 2000 were 30 m/y, 20% smaller than in the fluvial reach (Fig. 5A). The migration rate, between 2000 and 2010 (pre-flood), was 5 m/y. During the 2 months of the 2010 flood, the tide-influenced Indus channel migrated 198.5 m, or 4 m/d. A major upstream avulsion, north of Sukkur, greatly reduced the flow discharge in the main trunk river during the 2010 flood, so that the Indus only carried 43% of its upstream maximum discharge (Syvitski and Brakenridge, 2013).

The Indus Delta

The Pre-1869 or More Natural Delta State

The more natural Indus Delta is characterized by high river discharge, moderate tides and high wave energy conditions (Giosan et al. 2006). The delta shoreline advanced southwards and westwards at rates of between 4 and 30 m/year given the fluvial sediment delivery of over 400

Mt/y (Kazmi 1984); Milliman et al. (1984) suggest a pristine delivery rate between 270 and 600 Mt/y. The delta occupied an area of about 17,000 km^2 consisting of ~16 major tidal channels, mudflats and mangrove forest. The Indus River experienced tides inland as far as Thatta ~160 km upstream (Eisma 1998). The slope of the Indus River decreases by 50% (from 0.00008 to 0.00004) across the lower delta plain (Fig. 2).

Drainage patterns of the Indus Delta are sensitive to seismic activity, especially in the Kachchh portion of the Eastern delta. The western Rann has subsided in historical times, and tributaries of the Indus have dried up as the river distributaries changed their courses (Bilham, 1998; Iyengar et al, 1999; Thakkar et al., 2013). The 1819 Rann of Kachchh earthquake (Fig. 3) that caused more than 1500 deaths, had an estimated magnitude $7.7<Mw\leq8.2$, and was felt over a large part of India. Earthquake-induced subsidence formed Sindri Lake (Burnes, 1828) evident on all 19th century maps (see Suppl. matl.) and identifiable on recent imagery, and uplifted land approximately 80 km long, 6 km wide and ≤6 m high, which dammed the Puram River (Bilham et al. 2007). Prolonged aftershock activity continued for at least 50 years, including an estimated magnitude of 6.5 in 1846 (Bilham 1998). The 1819 earthquake also resulted in minor uplift north of Lukpat and subsidence in the delta west of the Kachchh mainland (Thakar et al 2012), and blockage of the important delta port of Shahbunder (Hughes, 1876).

In more pristine conditions, the Indus delta prograded tremendously, and Holmes (1968) reconstructed the active coastline at 325BC almost 100km inland from the current coast (an averaged rate of ~44 m/y). Progradation in the 19th century was over 200m/y near the active river mouth (Giosan et al., 2006). Figure 7 provides snapshots of the geolocated distributary channels of the Indus through this historical period. Consistently, these historical maps show a main channel coinciding with multiple other distributary channels in the delta plain. During the early map period between 1768 and 1811, the main Indus delta channel was along the western portion of the delta. The Jefferys (1768) map shows the main Indus channel following the paleo-Kalri

Branch, and a second major channel flowing along what is now the modern Indus southeast of Tatta (Thatta) and then along what is the paleo-Sattah branch (labeled Nala Sunkra; see suppl. matl.).

By 1804 (Rennell 1804; see suppl. matl.), the Nasirpur course (called the Dimtadee River on the map) flowed immediately to the north of the town of Nasirpur. The map of Arrowsmith (1804; see suppl. matl.) notes that the Indus flood season over the delta was in April, May and June, two months earlier than today, possibly indicating a greater contribution from the Himalaya. Pinkerton (1811; see suppl. matl.) states that the Indus River is navigable for 900km upstream. Steamships continued to ply the river as a cargo transport to Attock until replaced by railways in 1862 (Aitkin, 1907). The Baghar channel (Fig. 1) began to silt up in circa 1819. The Indus River then forged its main channel down its former Sattah Branch, but turned west, reaching the sea via the Ochito Branch (Fig. 1; Holmes 1968). Through the period 1830 - 1865 (SDUK 1833, Johnston 1861; see suppl. matl.) the main Indus delta channel was located along the modern Indus course, and numerous distributary channels were maintained both to the west and to the southeast (Fig. 7). On an 1833 map (SDUK 1833; see suppl. matl.) the tide is stated as reaching inland 111 km. By 1870-1910 (Letts 1883; see suppl. matl.), the main Indus had shifted further south and east while still maintaining flow to the western distributary channels (Fig. 7; also see Johnston and Johnston 1897 in the suppl. matl.). By 1922 (Bartholomew, 1922 suppl. matl. and Fig. 7), the Ochito River channel was the main branch, but this had largely been abandoned by 1944 (Fig. 7).

The post 1869 or Anthropocene Delta

The Indus channel is reduced to a single thread in its deltaplain, and the number of delta distributary channels has decreased during the 19^{th} century, from ~16 to 1 (Table 1, Fig. 6). The modern delta does not receive much fluvial water or sediment. There were zero no-flow days prior to the Kotri Barrage construction in 1955. After construction (c. 1975), up to 250 no-flow days per year occur. The average annual water and sediment discharges during 1931–1954 were 107 km^3 and 193 Mt, respectively. During the 1993 to 2003 period these rates dropped an order-of-magnitude to 10 km^3 and 13 Mt (Inam et al, 2007). The Indus discharge downstream of the Kotri Barrage is usually limited to only 2 months: August–September, with the sea now intruding the delta up to 225 km (Inam et al, 2007).

Abandoned Indus delta channels have been tidally reworked all along the coast (Figs. 8, 9). We mapped this evolution of delta channels using high-resolution imagery: 1) the 1944 topographic maps (USACE 1944; RMS location error ± 196m), 2) the 2000 SRTM/SWDB database (see suppl. matl.; RMS error ± 55m), and 3) LANDSAT imagery from 1978, 1989, 1990, 1991, 2000 (RMS location error between ± 32m and 196m). Imagery was selected to be representative of being part of the same astronomic tidal stage. By differencing the images we determined areas that had experienced sediment deposition or erosion on the tidal flats and new tidal channel formation (Fig. 9).

In the western Zone 1 (Fig. 8), the deltaic coast nearest Karachi, the 1944 tidal creeks show only minor amount of channel migration, a slight increase in tidal channel density in the outer flats, an increase in tidal channel density in the inner flats, and little to no increase in tidal inundation limits. Zone 1 had a net land loss of 148 km^2 incorporating areas of both erosion and deposition (Table 2, Fig. 8). Imagery in between 1944 and 2000 indicates that the shoreline saw episodic gains and losses. Giosan et al (2006) also noted that the shoreline in Zone 1 was relatively stable since 1954, but experienced progradation rates of 3 to 13 m/y between 1855 and 1954.

The west-central part of the delta (Zone 2 in Fig. 8) that includes the minor of two river mouths still functioning in 1944, shows larger changes: a >10 km increase in tidal inundation limits, the development of a dense tidal creek network including the landward extension of tidal channels, and shorelines that have both advanced and retreated. Zone 2 had a net loss of 130 km^2

(Table 2, Fig. 8). The Ochito distributary channel had been largely filled in with sediment since 1944.

In the south-central part of the delta (Zone 3 in Fig. 8) is the zone where 149 km^2 of new land area is balanced with 181 km^2 of tidal channel development (Table 2). The Mutni distributary channel, the main river mouth in 1944, and its associated tidal creeks, were filled in with sediment by 2000. Before the Mutni had avulsed to the present Indus River mouth, much sediment was deposited and the shoreline had extended seaward by more than 10 km (Figs. 8, 9). Large tidal channels were eroded into the tidal flats and tidal inundation was extended landward. We suspect that eroded tidal flat sediment contributed to the shoreline progradation in zone 3 of 150 m/y. Most of the progradation was prior to the 1975, in agreement with Giosan et al (2006).

The eastern Indus delta (Zone 4 in Fig. 8) experienced the most profound changes. Almost 500 km^2 of these tidal flats were eroded into deep and broad (2-3 km wide) tidal channels, balanced by < 100 km^2 of sediment deposited in older tidal channels (Fig. 8). Tidal inundation is most severe in zone 4 (Fig. 8).

In summary, during the 56-yr study interval parts of the Indus Delta lost land at a rate of 18.6 km^2/y, while other parts gained in area by 5.9 km^2/y, mostly in the first half of this period. During this time a stunning 25% of the delta has been reworked; 21% of the 1944 Indus delta was eroded, and 7% of the delta plain was formed (Table 2). To approximate these area loss or gain rates, to sediment mass we use 2 m for the average depth of tidal channels (see section C3 in Fig. 4). The erosion rate is then ~69 Mt/y, whereas the deposition rate is ~22 Mt/y, corresponding to a mean mass net loss of ~47 Mt/y. For the 72 y period 1931-2003, Inam et al. (2007) cite Pakistan Irrigation Department data indicating that 7.2 Gt of sediment was delivered to the Indus Delta at a mean rate of 100.6 Mt/y. Therefore if the delivery of 100 Mt/y of river sediment results in a net land loss equivalent of 47 Mt/y, then the pre-Anthropocene flux estimate of 250 Mt/y (Milliman et al. 1984) would result in an active Indus delta able to both aggrade and prograde seaward. The sediment budget remains qualitative, as it does not take into account subsidence across the delta, for lack of quantitative data. Satellite analysis suggests that there is significant sedimentation within the inner tidal flats of the Rann of Kachchh (Fig. 10), further complicating a full quantitative assessment.

Although part of the Rann of Kachchh (Lake Sindri south of the Allah Bund) underwent >1 m of incremental tectonic subsidence in 1819 it is not known whether slow secular subsidence occurs between earthquakes, either due to tectonic subsidence or sediment compaction. Tidal energy has been focused towards the eastern margins of the delta, apparently responding to changed hydraulic gradients or to the absence of sediments from the now inactive eastern distributaries. Evidently the sediment supply to Lake Sindri in the past 200 years has been insufficient to fill the tectonically induced basin since it remains a 20 x 30 km^2 basin, 1-2 m deep (Fig. 10). In contrast, the tidal flats in the western part of the Indus delta appear to be more stable, possibly protected from tidal and wave reworking of the shoreline by the absence of tectonic subsidence or possibly due to the presence of slow uplift.

The effects of the transition to the Anthropocene delta due to its much-increased abstraction of water upstream are pronounced and well documented: seawater intrusion, soil salinization, deforestation of mangroves, reduced supply of surface- and ground-derived drinking water, low irrigation flows, and greatly depleted fisheries. Shrimp production has decreased by 90% (Inam et al, 2007). The delta's mangrove forest, which covered ~2500 km^2, has been reduced by 60% (Kamal 2004). The degraded mangrove ecosystem is virtually mono-specific, comparatively stunted, with losses of about 2% per year **(**Asianics Agro-Dev. 2000). The increase in salinity during periods of low flow, and from the effects of upstream irrigation, has reduced the suitability of the delta for the cultivation of red rice, and for raising livestock. The herds of delta cattle, sheep and goats that once roamed the lower delta have disappeared; only herds of camel are to be found **(**Asianics Agro-Dev. 2000). The Anthropogenic Indus delta is hardly a true delta anymore, it receives too little water and sediment from the fluvial system, and tidal processes have taken control of the environment. In effect, it is a relict landform from pre-Anthropocene time.

Discussion and Conclusions

The hinterland of the pristine Indus river and delta system contributed annually 270 – 600 Mt of sediment towards its lowland floodplains and the ocean, creating a ~17,000 km^2 large delta over the Holocene that prograded up to 200 m/y until a century ago. The upstream river switched multiple times over the last 1000 years, occupying its entire 150 km-wide container valley. A multitude of channel belts aggraded and built 3-4 m high, several-km-wide, super-elevated ridges throughout the Indus plain. Detailed SRTM-InSAR topographic data highlight the positions of these large-scale ribbons. We also detect the topographic footprint of smaller scale crevasse splays and crevasse fingers shedding off the main channel. Some of these major river avulsions accompanied moderate earthquakes, and it is possible that a future earthquake could force the entire modern river system to abandon its current super-elevated course and reoccupy one of several lower elevation paleo-courses. As a result, river water would be diverted to a new path many tens or hundreds of km from its current channel, circumventing the extensive engineering works designed to constrain its current channels (see sections X4 and X8 in Fig. 4).

This river system became noticeable dominated by human action from 1869 onwards, with the systematic construction of continuous levees, which transformed the more natural drainage network into the world's largest irrigation system and reduced the sediment flux towards the Indus Delta to ~13 Mt/y. The engineering system harnessed the river into a narrow corridor of just 15 km wide. It appears that the present-day channel belt is super-elevated (~8m) more than paleochannel belts (3-4m). However, within this narrow floodplain corridor, the channel is still dynamic. This study also observed that the meander wavelength of the modern Indus is some 200% to 300% larger than for those historical Indus channels still evident in present-day landscape imagery. A positive change in meander wavelength is often associated with an increase in discharge (Hicken 1995, Chapter 7). It is possible as suggested earlier, that the impact of tight levees or bunds, is to both constrain and capture larger floodwaves along the modern Indus (Syvitski and Brakenridge, 2013). The period before levee construction saw numerous natural spillways that limited the flood discharge magnitude by releasing water into the dry desert.

This study reveals that the river sinuosity changed from 1.63 below Sukkur in 1944 to 1.82 in 2010 (pre-flood conditions). After the 2010 river flood, the sinuosity decreased to 1.71. The centerline of the main channel migrated lateral 1.95 ± 0.2 km over the same period (or 36 m/y) with an astonishing average of 339 m migration in just 52 days comparing pre and post flooding main channel centerline positions. This data suggests that the 66 year channel migration total perhaps occurred largely during only 8 flood events: peak events occurred in 1950, 1956, 1957, 1973, 1976, 1978, 1988, 1992 and 2010 (Hashmi 2012). These migration rates occur despite the extensive system of artificial levees, and the erosion poses acute danger to people, livestock and infrastructure during the floods, and mandates considerable maintenance and repair after floods. We speculate that this damage will only exacerbate with a continued aggradation in the main channel, much like the repetitive cycle of the historical Yellow River levee breaches and floods (Chen et al., 2012).

In summary, the anthropogenic impacts upstream and tectonic controls downstream have led in a short time to the following morphological changes to the delta:

1) The number of distributary channels reduced from 17 in 1861 to just 1 in 2000.
2) A change has occurred from a fluvial-dominated delta system to a more tidally controlled system, with reworking of the abandoned delta channels along the coast. The main portion of the delta is now a relict landform.
3) Tectonic -induced subsidence at the eastern part of the delta and stable conditions to possible uplift in the west have resulted in accelerated coastal erosion at the Rann of Kachchh area (eastern part of the delta).

4) Since 1944, the delta has lost 12.7 km^2/y of land; 25% of the delta has been turned over, 21% of the delta was eroded and 7% of new land was added. This equals an annual sediment loss of ~47Mt, assuming 2m depth average tidal channels.

We speculate that the deterioration of the Indus delta from its previous state was initiated and is maintained by human-caused perturbations; mainly, the upstream use of water and the trapping of the associated sediment flux. According to our findings, self-regulating processes have largely not buffered these changes; instead, some have indeed initiated self-enhancing mechanisms (e.g., changes in river form in response to floods). It is unlikely that the river-delta system, now dominated by tidal processes, could be converted back to its pre-Anthropocene state. Yet the present system exhibits trends that, if left unmitigated, will affect sustained habitability by the human population.

References

Ahmed, M., Cook, E., 2011. Upper Indus River-flow reconstruction using tree- rings: implications for agriculture and hydroelectricity. Pakistan-US Science and Technology Cooperation Program Final Report. National Academy of Sciences, Development Security and Cooperation, Policy and Global Affairs 14.

Aitkin, E.H., 1907. Gazetteer of the Province of Sind. London.

Andree, R., (Times, London) 1895. Central Asia and India. The Times of London Publ., Scale 1: 10,000,000, Page No: 77-78.

Arrowsmith, A., 1804. Middle Sheet, Map of India. A. Arrowsmith Publ., London, Scale 1: 1,759,575.

Asianics Agro-Dev. International (Pvt.) Ltd., 2000. Tarbela Dam and related aspects of the Indus River Basin, Pakistan. Final Report World Commission on Dams, Cape Town, pp. 212.

Bartholomew, J., 1922. Composite of Section maps of India. The Edinburgh Geographical Institute, London: The Times, p. 56-60; Scale 1: 4,000,000.

Bendick, R., Bilham, R., Fielding, E., Gaur, V.K., Hough, S., Kier, G., Kulkarni, M. N., Martin, S., Mueller, K., Mukul, M., 2001. The January 26, 2001 "Republic Day" Earthquake. India. Seism. Res. Lett. 72(3) 328-335.

Bilham, R., 1998. Slip parameters for the Rann of Kachchh, India, 16 June 1819 earthquake, quantified from contemporary accounts. In: Stewart I.S. & Vita-Finzi C. Coastal tectonics. Special Publ. 146. London: Geological Society. pp. 295–319.

Bilham, R., Lodi, S., Hough, S., Bukhary, S., Khan, A.M., Rafeeqi S.F.A., 2007. Seismic Hazard in Karachi, Pakistan: Uncertain Past, Uncertain Future. Seismological Research Letters 78, 601-613.

Bilham, R., Bendick, R., Wallace, K., 2003. Flexure of the Indian Plate and intraplate earthquakes. Proc. Indian Acad. Sci. (Earth Planet Sci.), 112(3) 1-14.

Bilham, R., Lodi, S., 2010. The door knockers of Mansurah,: Strong shaking in a region of low perceived seismic risk, Sindh, Pakistan. In: M. Sintubin, I.S. Stewart, T.M. Niemi, E. Altunel, (Eds.) Geol. Soc. America Special Paper 471, 29-37.

Biswas, S. K., 2005. A review of structure and tectonics of Kachchh basin, western India, with special reference to earthquakes. Current Science 88(10): 1592-1600.

Bodin, P., Horton S., 2004. Source Parameters and Tectonic Implications of Aftershocks of the Mw 7.6 Bhuj Earthquake of 26 January 2001. Bull. Seismological Society of America 94(3) 818–827.

Burnes, A., 1828. A Memoir and Supplementary Memoir of a map of the Eastern Branch of the Indus. Fol., Bombay. Transcript from a handwritten text with map. LDGSL 767 Geological Society of London.

Chen, Y., Syvitski, J.P.M., Gao, S., Overeem, I., Kettner, A.J., 2012. Socio-economic impacts on Flooding: a 400 year history of the Yellow River, China. Ambio, 41 (7) 682-698.

Clift, P.D., Giosan, L., 2013. Sediment Fluxes and Buffering in the Post-Glacial Indus Basin. Basin Research, online ahead of print.

Fahlbusch, H., Schultz, B., Thatte, C.D., 2004. The Indus Basin: History of Irrigation, Drainage and Flood Management. International Commission on Irrigation and Drainage, New Delhi, India.

Giosan, L., Clift, P.D., Macklin, M., Fuller, D., Constantinescu, S., Durcan, J.A., Stevens, T., Duller, G.A.T., Tabrez, A.R., Gangal, K., Adhikari, R., Alizai, A., Filip, F., VanLaningham, S., Syvitski, J.P.M., 2012. Fluvial Landscapes of the Harappan Civilization. Proceedings of the National Academy of Science 109, 26.

Giosan, L., Constantinescu, S., Clift, P.D., Tabrez, A.R., Danish, M., Inam, A., 2006. Recent morphodynamics of the Indus delta shore and shelf. Continental Shelf Research 26, 1668–1684.

Haig, M. R., 1894. The Indus Delta Country; A memoir chiefly on its ancient geography and history. Kegan Paul, Trench & Tru□bner Publ., London, pp. 148.

Hannon M., 2011. Exploring predictive relationships of fluvial morphology using Shuttle Radar Topography Mission data. M.Sc. Thesis, U. Colorado, Boulder CO, pp. 80.

Haq, B.U., 1999. Past, Present and Future of the Indus Delta. In: A. Meadows & P. Meadows (Eds.), The Indus River (Biodiversity, Resources, Humankind), Oxford University Press, pp. 132-140.

Hashmi, H.N. Siddiqui, Q.T.M., Ghumman, A.R., Kamal, M.A., Mughal, H.R., 2012. A critical analysis of 2010 floods in Pakistan. African J Agricultural Res 7, 1054-1067.

Hicken, E.J., (Ed.) 1995. River Geomorphology, John Wiley & Sons, 295 pp.

Holmes, D.A., 1968. The recent history of the Indus. Geographical J. 134: 367–382.

Hughes, A. W., 1876. A Gazetter of the province of Sind. London, pp 980.

ICOLD 1998. World Register of Dams. International Commission on Large Dams, Paris, France (1984, 1988, 1998).

Inam, A., Khan, A.T.M., Amjad, S., Danish, M., Tabrez, A.R., 2004. Natural and man made stresses on the stability of Indus deltaic eco-region. Extended Abstract, The 5th Intl. Conf. Asian Marine Geology, Bangkok, Thailand (IGCP475/APN).

Inam, A., Clift, P., Giosan, L., Tabrez, A.R., Tahir, M., Rabbani, M.M., Danish, M., 2007. The Geographic, Geological and Oceanographic Setting of the Indus River. In: A. Gupta (Ed.), Large Rivers: Geomorphology and Management. John Wiley & Sons, pp. 333-346.

Ivory S.J., Lézine A.M., 2009. Climate and environmental change at the end of the Holocene Humid Period: A pollen record off Pakistan. Comptes Rendus Geoscience 341, 760-769.

Iyengar, R.N., Sharma, D., Siddiqui, J.M., 1999. Earthquake history of India in medieval times. Indian J of History of Science 34, 181-236.

Jefferys, T., 1768. Composite of the East Indies with the roads. Robert Sayer Publ., London, pp. 24-25; Scale 1: 2,600,000.

Johnston A.K., 1861. India, northern sheet. William Blackwood & Sons Publ., Edinburgh, p. 32, Scale 1:4,457,000.

Johnston, W., Johnston A.K. (Ltd.), 1897. Bombay (North) and Baroda, Bombay South. Edinburgh; London 1:3,990,000, p. 102-103.

Jorgensen, D.W., Harvey, M.D., Schumm, S.A., Flam, L., 1993. Morphology and Dynamics of the Indus River: Implications for the Mohen jo Daro site. In: Shroder, J.F., Jr (Ed.), Himalaya to the Sea. Routledge, London, 228-326.

Kamal, S., 2004. Area Water Partnerships (AWPs) and their Potential for Community-based Action in IWRM, International Symposium on Community Based Approaches for Integrated Water Resources Management, Islamabad, Feb. 16-17, 2004.

Kazmi, A.H., 1984. Geology of the Indus Delta. In: Haq, B.U., Milliman, J.D. (Eds.), Marine Geology and Oceanography of Arabian Sea and Coastal Pakistan. Van Nostrand Reinhold, New York, pp. 65–70.

Knighton, D., 1998. Fluvial Forms and Processes: A New Perspective. Hodder Arnold Publishers.

Kovach, R. L., Grijalva, K., Nur, A., 2010. Earthquakes and civilizations of the Indus Valley: a challenge for archaeologists, Geol. Soc. Amer. Sp. Paper 471, 119-127.

Lal BB and Gupta SP Eds., 1984. Frontiers of the Indus Civilization, (Indian Archaeological Society jointly with Indian History & Culture Society, London).

Lambrick, H.T., 1964. Sind: A General Introduction. Sindhi Adabi Board, Hyderabad, pp. 289.

Lapie, M.P., 1829. Carte de l'Inde en deca et au dela du Gange. Chez Eymery Fruger et Cie. Publ., Paris, publication date1833, Scale 1:10,100,000.

Letts, A., 1883. Statistical & general map of India. No. 5. Letts, Son & Co. Limited, London. p 89; Scale 1: 2,217,600

Memon, A.A., 2005. Devastation of the Indus River Delta. Proceedings, World Water & Environmental Resources Congress 2005, ASCE, Environmental and Water Resources Institute, Anchorage, Alaska (Expanded version).

Milliman, J.D., Quraishee, G.S., Beg, M.A.A., 1984. Sediment discharge from the Indus River to the ocean: past, present and future. In: Haq, B.U. and Milliman, J.D. (Eds.), Marine Geology and Oceanography of Arabian Sea and Coastal Pakistan. Van Nostrand Reinhold, New York, pp. 66–70.

Mughal M.R., 1997. Ancient Cholistan. Archaeology and Architecture (Ferozsons, Lahore).

Oldham, C.F., 1893. The Saraswati and the lost river of the Indian desert. J. Royal Asiatic Soc. (New Series) 34: 49-76.

Oldham, R.D., 1887. On probable changes in the geography of the Punjab and its rivers: an Historico-geographical study. J. Asiatic Soc. Bengal **55**(2), 322-343.

Panhwar M.H., 1981. The art of map making and some rare maps of the South Asia and Sindh 140 AD to 1808 AD. J Sindh Quarterly IX, 39-54.

Panhwar, M. H., 1969. Ground Water in Hyderabad & Khairpur Divisions. Directorate of Agriculture, Hyderabad Region, pp. 217.

Pinkerton, J., 1811. Hindostan, Cadell & Davies Publ., London, p 34, Scale 1:6,250,000

Rennell, J., 1804. A new map of Hindoostan from the latest authorities. North half. Published by Laurie & Whittle, 53, Fleet Street, 12th May, 1794. 2nd edition. Corrected 1804. Scale 1:2,500,000.

Rizvi, S.H.N., Ali, A., Naeem, S.A., Tahir, M., Baquer, J., Saleem, M., Tabrez, S.M., 1988. Comparison of the physical properties of seawater offshore the Karachi coast between the northeast and southwest monsoons. In: Thompson, M., Tirmizi, N.M. (Eds.), Marine Science of the Arabian Sea. Proc. Intl. Conf., American Institute of Biological Sciences, Washington, DC.

Rochette, de la, L.S., 1800. Hind, Hindoostan, or India. William Faden Publ., London, p. 42, Scale 1:5,650,000

Schelling, D. D., 1999. Frontal structural geometries and detachment tectonics of the northeastern Karachi arc, southern Kirthar Range, Pakistan, Geol. Soc. Amer. Sp. Pap. 328, 287-302.

Schumm, S.A., Dumont, J.F., Holbrook, J.M., 2002. Active Tectonics and Alluvial Rivers. Cambridge University Press, Cambridge UK, 276 pp.

SDUK Society for the Diffusion of Useful Knowledge, 1833. India V. Chapman & Hall, London, publication date 1844, p. 101, Scale 1:2,200,000 Maps of the Society for the Diffusion of Useful Knowledge. Vol. 1.

Siddiqui, M.N., Jamil, Z., Afsar, J., 2004. Monitoring changes in riverine forests of Sindh-Pakistan using remote sensing and GIS techniques. Advances in Space Research 33, 333–337.

Siddiqui, Z.A., Shakeel, M., 1995. Monitoring and mapping of river course changes in the river Indus using Landsat MSS images. Asian Pacific Remote Sensing J. 8, 101–105.

Stein, M. A., 1942. A survey of ancient sites along the 'lost' Saraswati River. Geogr. J. 99, 173-82.

Syvitski J.P.M., Hannon M.T, Brakenridge R., 2011. The Great Indus Flood of 2010. The 7th IAHR Symposium on River, Coastal and Estuarine Morphodynamics, Sept. 6-8, 2011, Tsinghua University, Beijing, China.

Syvitski, J.P.M, Brakenridge, G.R., 2013. Causation and avoidance of catastrophic flooding along the Indus River, Pakistan. GSA Today 23, 4-10.

Syvitski, J.P.M., 2008. Deltas at Risk. Sustainability Science 3, 23-32.

Syvitski, J.P.M., Kettner, A.J., Hannon, M.T., Hutton, E.W.H., Overeem, I., Brakenridge, G.R., Day, J., Vörösmarty, C., Saito, Y., Giosan, L., Nicholls, R J., 2009. Sinking deltas due to human activities, Nature Geoscience 2, 681-689.

Syvitski, J.P.M., Saito, Y., 2007. Morphodynamics of Deltas under the Influence of Humans. Global and Planetary Changes 57, 261-182.

Syvitski, JPM, Overeem, I., Brakenridge, G.R.; Hannon, M.D., 2012. Floods, Floodplains, Delta plains — A Satellite Imaging Approach. Sedimentary Geology 267/268, 1-14.

Szeliga, W., Bilham, R., Kakar, D.M., Lodi, S.H., 2012. Interseismic strain accumulation along the western boundary of the Indian subcontinent. J. Geophys. Res., 117, B08404.

Thakkar, M. G., Nganom, M., Thakkar, P.S., Juyal, N., 2013. Terrain response to the 1819 Allah Bund earthquake in western Great Rann of Kachchh. Current Science 103, 2008-2012.

U.S. Army Corps of Engineers, 1944. Survey of India Maps, Prepared by Army Map Service (GPDE), Washington DC Scale: 1:250,000. (1): NG42-2, Series U502, Title SUKKUR, Pakistan; (2) NG42-3, Series U502, Title Mirpur Mathelo, Pakistan & India; (3) NG42-11, Series U502, Title Mirpur Khas, Pakistan; (4) NG42-15, Series U502, Title Islamkot, Pakistan; (5) NF42-02, Series U502, Title Lakphat, Pakistan & India; (6) NG42-13, Series U502, Title Karachi, Pakistan; (7) NG42-14, Series U502, Title Tatta, Pakistan & India; (8) NG42-10, Series U502, Title Hyderabad, Pakistan; (9) NG42-06, Series U502, Title Nawabshah, Pakistan.

U.N., 2012. Population Division of the Department of Economic and Social Affairs of the United Nations Secretariat, World Population Prospects: The 2012 Revision, http://esa.un.org/unpd/wpp/index.htm

Wells, J.T., Coleman, J.M., 1984. Deltaic morphology and sedimentology, with special reference to the Indus River elta. In: Haq, B.U., Milliman, J.D. (Eds.), Marine Geology and Oceanography of Arabian Sea and Coastal Pakistan. Van Nostrand Reinhold, New York, pp. 85–100.

Wilhelmy, H., 1966. Der Wandernde Strom: Studien zur Talgeschichte des Indus. Erdkune XX, 265-276

Wilhelmy, H., 1967. The shifting river; studies in the history of the Indus valley. Universitas 10, 53–68.

Acknowledgements

JS and AK were funded through the Land Cover / Land Use Change program of the U.S. National Aeronautics and Space Administration (NASA) under Grant No. NNX12AD28G. RB was funded by NSF grant EAR 0739081, MH and IO received support from ConocoPhillips.

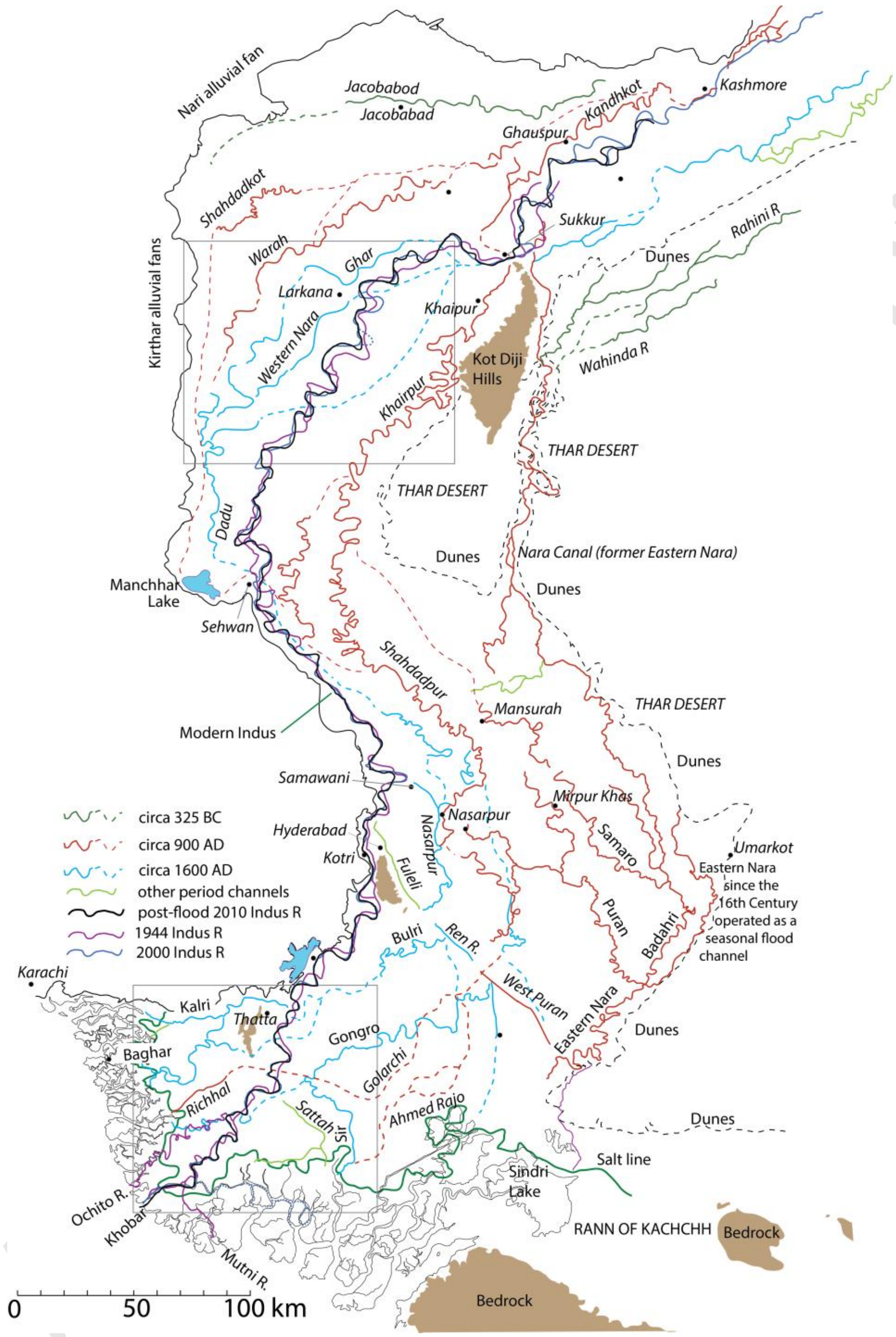

Figure 1. General map of the Indus floodplain and delta; towns/cities used in text are identified with geographic features and the salt (green) line of the Indus Delta. The 2000 position of the Indus River (dark blue) is from SRTM/SWBD data, the 1944-Indus (purple) is from USACE data, and the 2010 post flood image (black) is from Landsat 5 imagery. Paleo-Indus channels are from satellite imagery; their names and age are from Holmes 1968. Dellta and floodplain boxes represent SRTM data locations of Figures 5A and 5B.

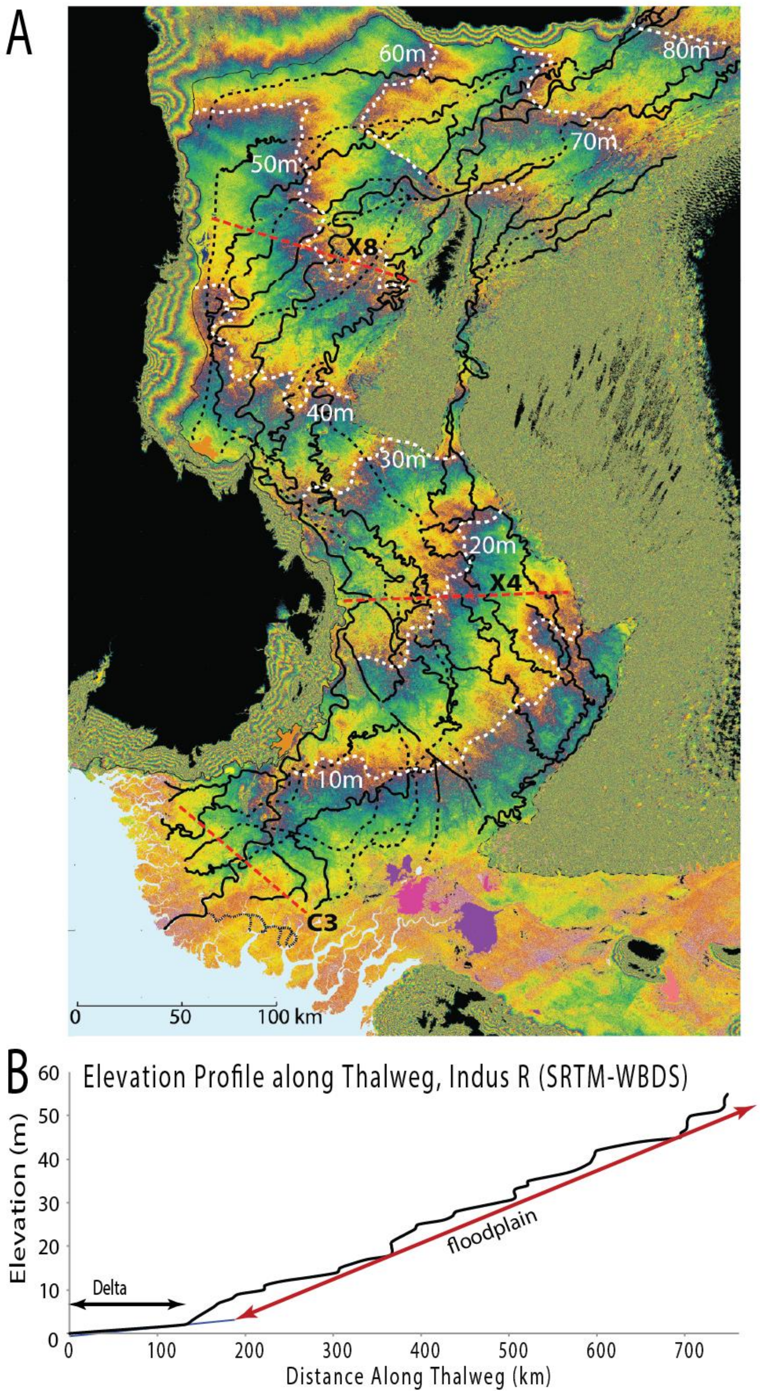

Figure 2. A) Floodplain imaged with SRTM C-band InSAR — colors change every 1 m of vertical elevation and cycle every 10 m; black elevations are >100 m. Superimposed on the digital elevation model are the modern (2000) and paleo Indus river channels as differentiated in Figure 1. Also superimposed are the generalized 10m elevation contours as a visual aid. Figure 4 profile locations are in dashed red and labeled. B) Elevation profile of the Indus thalweg using SRTM-WBDS data. Note the very different slopes between the Delta portion and the Indus floodplain portion. Also note the sediment waves (steps) seen in the river profile.

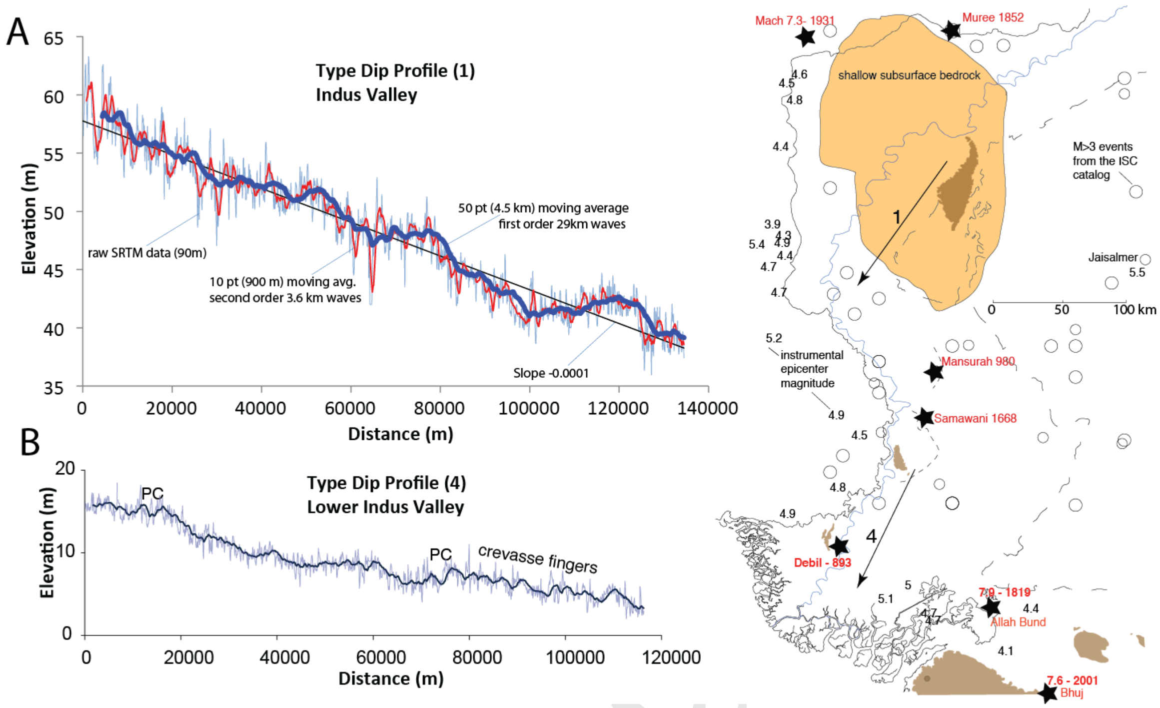

Figure 3. DEM-based dip profiles generated from SRTM data (see Fig. 2) showing raw 90 m profiles, 50 point (4.5 km) moving average profiles showing first order 29 km sediment waves, and 10 point (900 m) moving average profiles showing second order 3.6 km waves. The raw SRTM 90m signature is itself based on 30m data averaged by NGA around the mid-pixel. This raw signature shows 3 – 8 m vertical fluctuations with a horizontal wavelength of 1.8 km off of the linear down-valley slope of 1:10000 (5.7 x 10^{-3} degrees). Also identified on the profiles are the crevasse fingers seen in Fig. 2 and the paleo-channels (PC) identified in Fig. 1 and 2. The inset map after Bilham et al, 2010, shows the zone of shallow subsurface bedrock centered at Sukkur, along with instrumental seismic activity to 2001 denoted by numerical magnitudes, less accurate M<3 epicenters by open circle. Damaging earthquakes both historical (893 -Kovach et al., 2010, c. 980, 1668, & 1819 for which magnitudes are inferred or unavailable) and instrumental (1930-2001 indicated by stars with magnitudes).

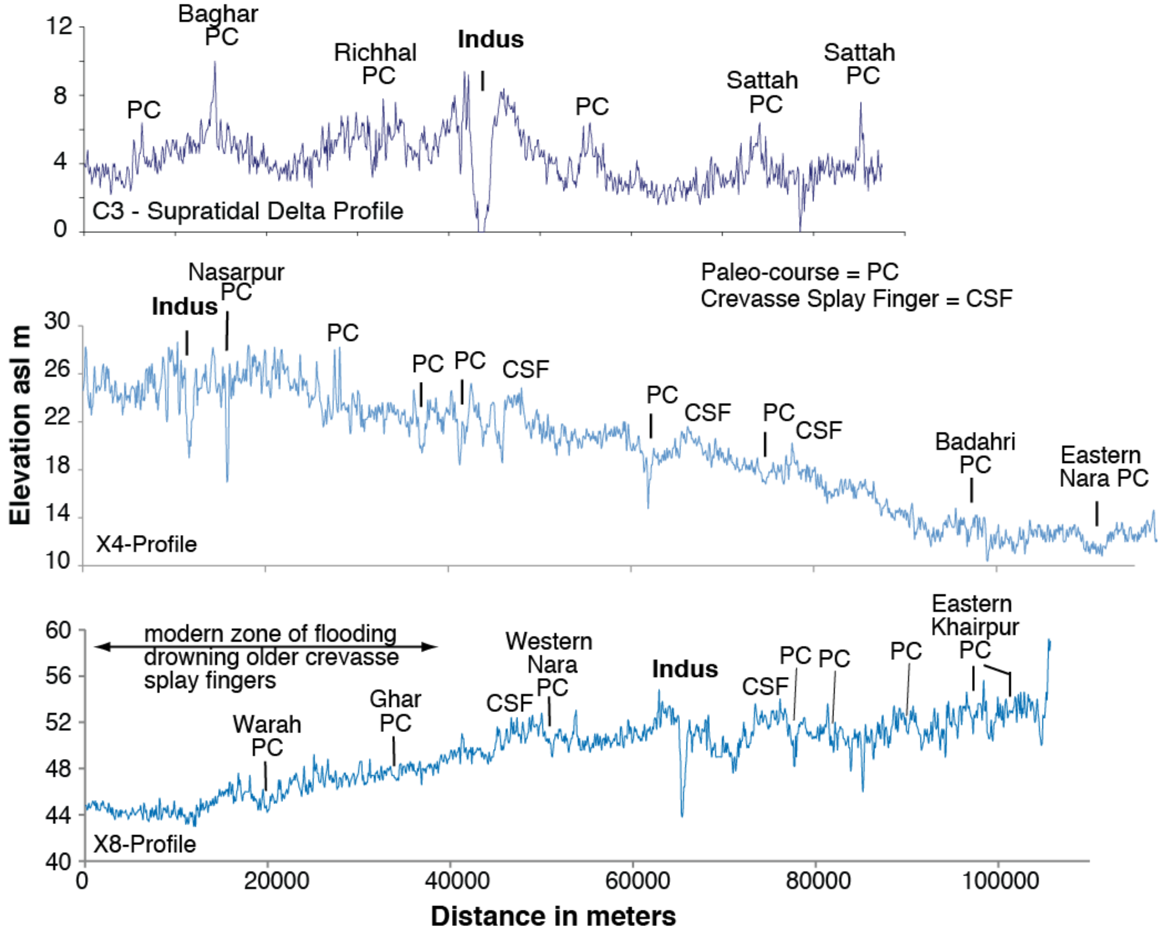

Figure 4. Cross-valley strike profiles (Fig. 2 for map location) of elevation across the paleo Indus floodplain are based on 90m SRTM DEM. The inset shows paleo and modern channels, the modern floodplain and the strike sections). Profiles are comprised of the average of five 90m-spaced parallel profiles to eliminate spurious roughness features. At section C3, the Indus is well expressed as an 8 m deep channel, and other paleo channels are super-elevated above the surrounding floodplain similar to crevasse splays. For sections further up-valley, paleo channels are cut into the floodplain between 1 and 4 m. The Nasarpur Channel (e.g. X4) and the Shahdadpur Channel are the same relief and dimensions as the modern Indus. Other paleo channels such as the Eastern Khairpur (e.g. X8), and Eastern Nara (e.g. X4) are smaller, and many others are much smaller.

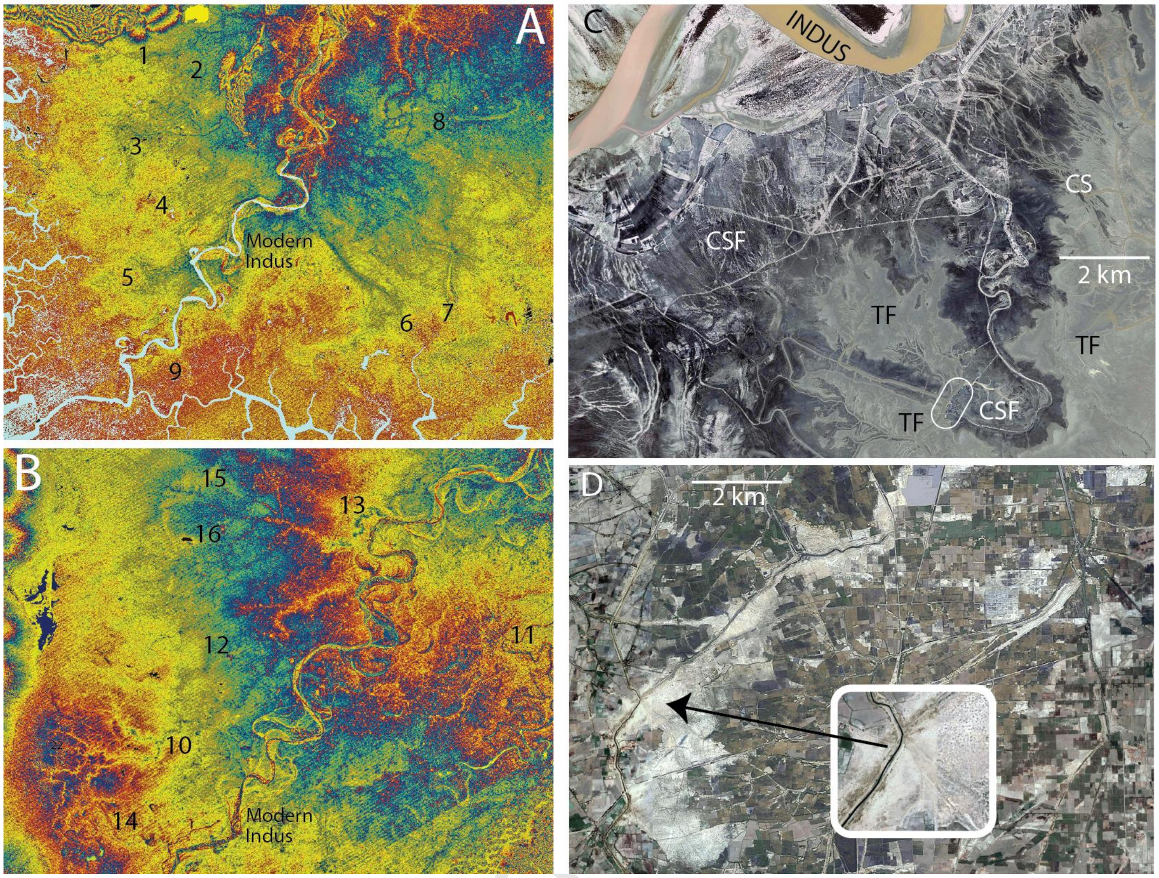

Figure 5: SRTM images of the A) Indus Delta, <13m above sea level, and B) the Indus or Sindh floodplain between 39 and 55m above sea level (see Fig. 1 for locations). Colors change every m; color pattern repeats every 10 m; light blue is mean sea level. A) 1-Kalri paleo-branch; 2-Malaki paleo-branch; 3-Baghar paleo-branch; 4-Richhal paleo-branch; 5-Orchito paleo-branch; 6-Sattach paleo-branch; 7-Sir paleo-branch; 8-Gongro paleo-branch; 9-relatively recent splay off of the Indus (see Figure 5C). B) 10-paleo Dadu channel; 11-paleo Khairpur channel; 12-paleo Western Nara channel; 13-paleo Ghar channel; 14-paleo Jacobabad or Shahdadkot channel partially buried in flood deposits of paleo Lake Manchur); 15-paleo Warah channel; 16-crevasse splay fingers off of the paleo Ghar channel now occupied by irrigation canals. C) 2007 Digital Globe image (inverted for contrast) of an elongated Indus crevasse splay finger (CSF) that has become eroded from tidal action (see oval). D) 2008 Digital Globe image of a paleo crevasse-splay levee likely from the paleo-Gongro. A recent irrigation canal has been cut into the levee deposit. The inset shows erosional channels cutting across the splay levee from canal floodwaters.

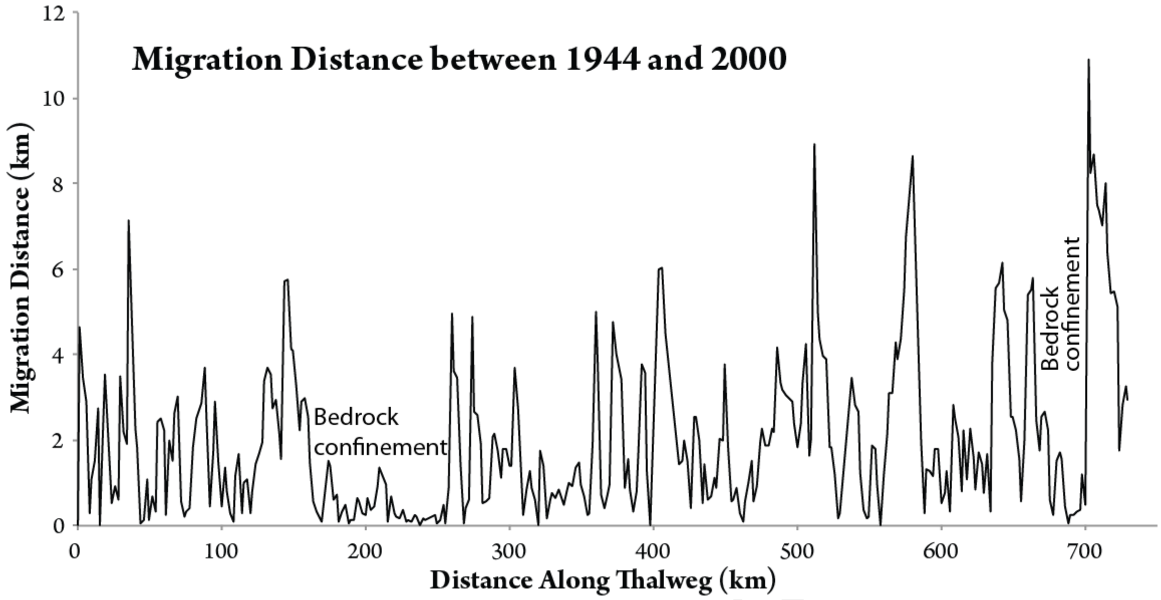

Figure 7. Distance between the position of the 1944 Indus Channel (USACE 1944) and the 2000 channel position (90 m-resolution SRTM, see Table 1). Large areas of limited migration are due to channel pinning by bedrock valley confinement.

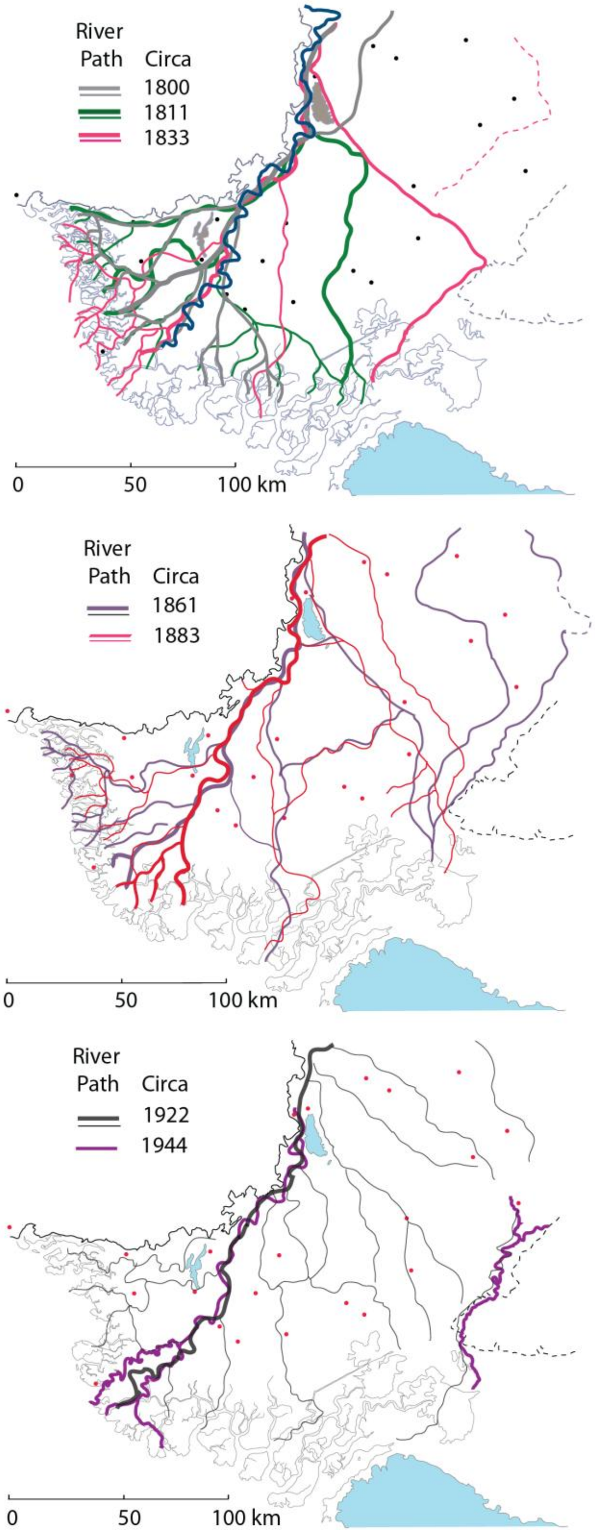

Figure 6. Geo-located distributary channels of the Indus from 1800 to 1944, using historical maps (cf. Table 1).

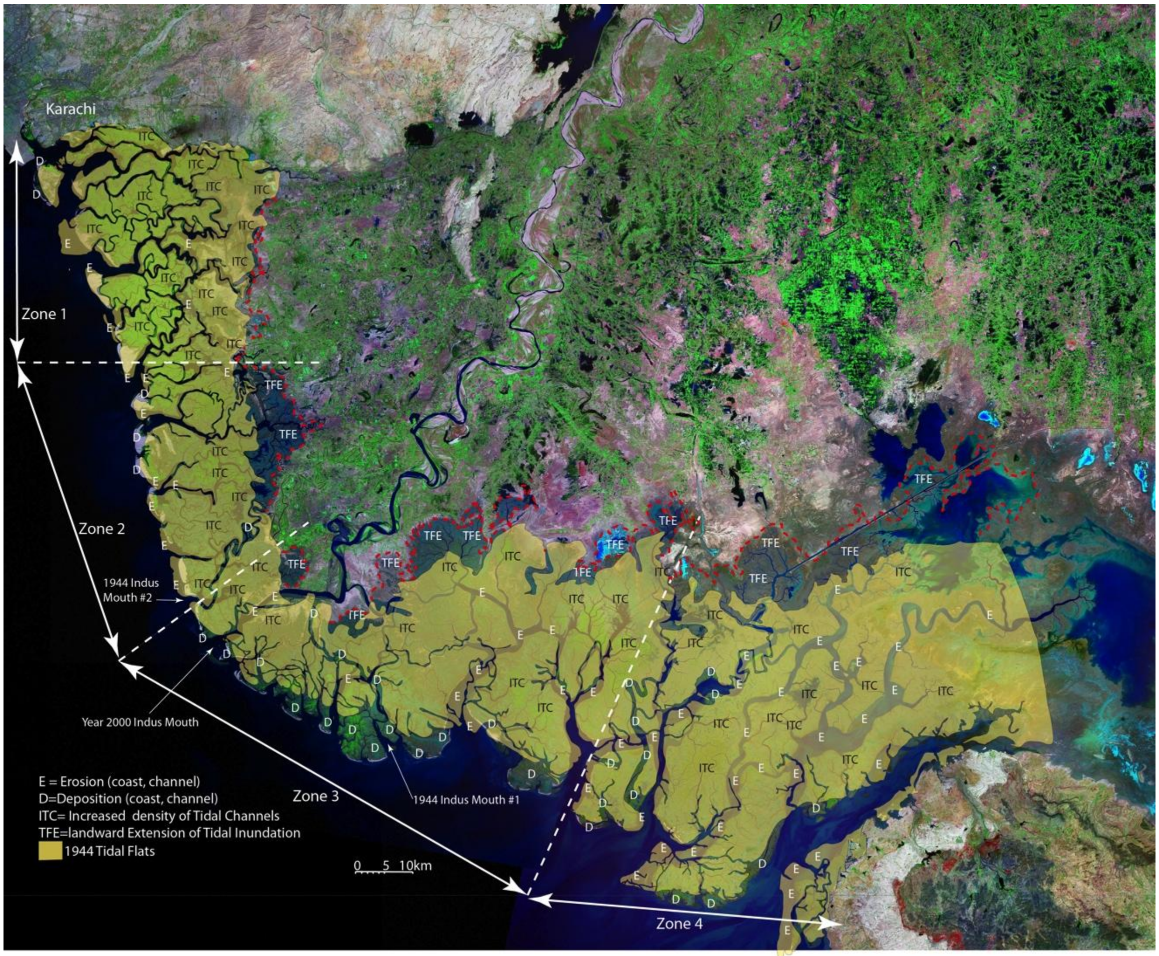

Figure 8. The background image is from a LANDSAT 7 composite of the Indus Delta from the year 2000. Superimposed is the circa 1944 USACE high-resolution maps of the Indus Delta (see suppl. matl.) shown in transparent yellow. The year 2000 tidal channels can be seen through the 1944 overlay. The letter E indicates areas of post 1944 erosion. The letter D indicates areas of post 1944 sediment deposition. ITC indicate increased density of tidal channels since 1944. TFE indicates areas with tidal inundation expansion since 1944. See text for details.

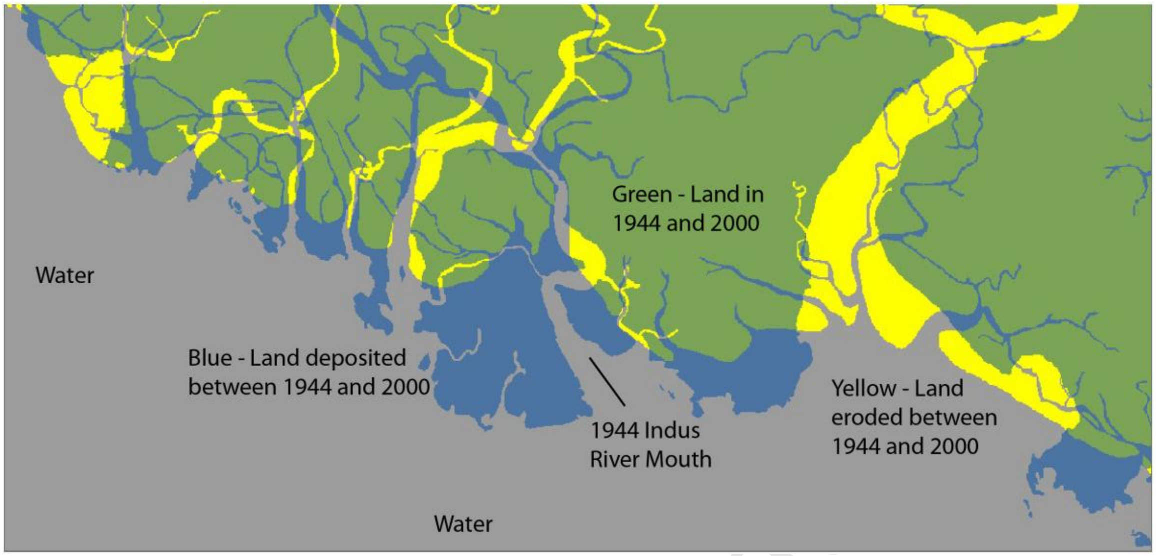

Figure 9: Small section of the Indus Delta showing the 1944 river mouth of the Indus (see Fig. 8). Yellow --- areas of net erosion between 1944 and 2000, blue --- areas of deposition, and green areas with no change.

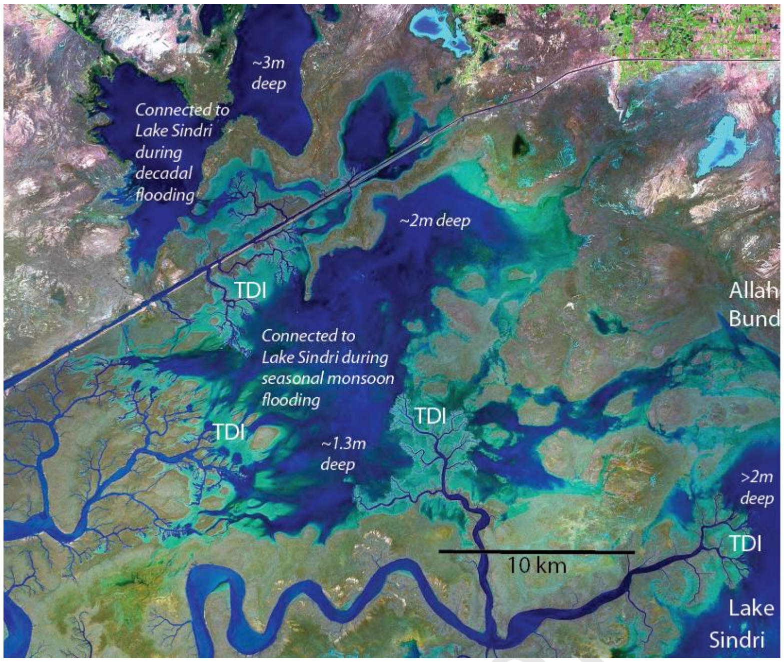

Figure 10: Easter portion of the Indus Delta showing where sediment is tidally being pushed into the subsiding Lake Sindri (Pakistan and India) as tidal delta infill (TDI). Also shown is the uplifted Allah Bund from the earthquake of 1819.

Table 1: *Historical map information used in the construction of Fig. 5 (also see suppl. matl.) indicating the number of river mouths (12-17) and this decrease from 1900 into modern times where only one mouth of significance remains. The main historical channels are named. The RMS geo-location error is in m.*

Year	**River Mouths**	**Major Outlets**	**Outlet Name**	**Map Scale Reference**		**RMS Error (m)**
1768	??	2	paleo-Kalri, Nala Sunkra	1: 2,600,000	Jefferys, 1768	unknown
1800	12	1	paleo-Baghar	1:5,650,000	De la Rochette, 1800	unknown
1804	16	3	Darraway, Ritchel, Nulla Sunkra	1:1,759,575	Arrowsmith, 1804	unknown
1811	15	4	Darraway, Fette, Churar, Chunarsatre	1:6,250,000	Pinkerton, 1811	5195
1833	14	3	paleo-Baghar, Sala, Puran	1:2,200,000	SDUK, 1833	6208
1861	17	1	Indus (Khediwarri)	1:4,457,000	Johnston, 1861	4158
1883	17	2	Baghar, Kookiwari	1: 2,217,600	Letts, 1883	3828
1897	14	4	Baghar, Uchto, Vatho, Kookiwari, Sir	1:3,990,000	Johnston, 1897	4061
1922	8	1	Indus	1:4,000,000	Bartholomew, 1922	3410
1944	6	2	Ochito, Mutni	1:250,000	USACE, 1944	196
2000	1	1	Indus	1:90,000	Farr et al., 2007	55

Table 2: *Area of the 1944 Indus Delta tidal flat, with zones identified with referring to the Indus Delta Zones (cf Fig. 8).*

Zones	Total 1944 Area km^2	Area with No Change km^2	2000-1944 Erosion Area km^2	2000-1944 Deposit Area km^2	Total 2000 Area km^2
1	953	693	204	56	805
2	771	588	167	37	641
3	1159	810	181	149	1127
4	2073	1485	492	96	1677
T. Area	**4956**	**3575**	**1043**	**338**	**4251**
Load Mt/y	**-**	**-**	**68.9**	**22.3**	**-**